Korean Journal of Remote Sensing, Vol.34, No.1, 2018, pp.75~87
http://dx.doi.org/10.7780/kjrs.2018.34.1.5

ISSN 1225-6161 (Print)
ISSN 2287-9307 (Online)

Article

Inundation Hazard Zone Created by Large Lahar Flow at the Baekdu Volcano Simulated using LAHARZ

Sung-Jae Park*, and Chang-Wook Lee*†

*Division of Science Education, Kangwon National University

Abstract : The Baekdu volcano (2,750 m a.s.l.) is located on the border between Yanggando Province in North Korea and Jilin Province in China. Its eruption in 946 A.D. was among the largest and most violent eruptions in the past 5,000 years, with a volcanic explosivity index (VEI) of 7. In this study, we processed and analyzed lahar-inundation hazard zone data, applying a geographic information system program with menu-driven software (LAHARZ) to a shuttle radar topography mission 30 m digital elevation model. LAHARZ can simulate inundation hazard zones created by large lahar flows that originate on volcano flanks using simple input parameters. The LAHARZ is useful both for mapping hazard zones and estimating the extent of damage due to active volcanic eruption. These results can be used to establish evacuation plans for nearby residents without field survey data. We applied two different simulation methods in LAHARZ to examine six water systems near Baekdu volcano, selecting weighting factors by varying the ratio of height and distance. There was a slight difference between uniform and non-uniform ratio changes in the lahar-inundation hazard zone maps, particularly as slopes changed on the east and west sides of the Baekdu volcano. This result can be used to improve monitoring of volcanic eruption hazard zones and prevent disasters due to large lahar flows.

Key Words : Baekdu volcano, VEI, Hazard, Lahar

1. Introduction

The Baekdu volcano has a peak of 2,750 m and is located on the Changbai Mountain Range, which forms the border between South Korea and China (Yun and Choi, 1996). Baekdu volcano's high altitude leads to primary damage by lava flows following eruption, as well as secondary damage due to flooding and lahars from the caldera lake at the top of the mountain. Lahars flow throughout volcanic eruption, and are fed by snow, ice, or lakes at the top of the volcano; speeds can reach 65 km/h over a distance of 80 km (Newhall *et al*., 1997b). A lahar constantly changes its speed and volume, depending on the region through which it flows, and can increase if the lahar flows into a river or lake instead of a valley. As the lahar moves away from the volcano, it slows down at lower slopes and its volume decreases; however, on steep slopes, its speed

Received January 30, 2018; Revised February 8, 2018; Accepted February 13, 2018; Published online February 23, 2018
† Corresponding Author: Chang-Wook Lee (cwlee@kangwon.ac.kr)

can exceed 200 km/h (U.S.G.S. Volcano Hazards Program-Lahars). Lahars exhibit fluid flow, but retain some solid properties, resulting in enormous loss of life and property on impact (Schilling, 1998). For example, on June 15, 1991, the volcanic eruption of the Pinatubo volcano in the Philippines, which had a volcanic explosivity index (VEI) of 6, caused damage to low-lying villages due to large amounts of volcanic ash and about 3 km^3 of lahar. According to a 1996 survey, sediments from the Pinatubo volcano eruption were at temperatures near 500°C in 1991, causing explosions upon contact with rivers or groundwater (Newhall *et al*., 1997a). Since 1991, the volcanic potential of the Pinatubo volcano lahar has led to the development of the first lahar monitoring system. Early detection by this system could prevent hundreds of casualties (Newhall *et al*., 1997b). Past investigations of lahar flood areas have generally been conducted by examining the sediments in the area and estimating the locations and ages of lahar sediments. However, most volcanoes are difficult to access, and there is a lack of lahar data and sediment observations for some volcanoes (Schilling, 1998). In the case of the Baekdu volcano, it is difficult to predict the extent of damage based on past events due to the lack of quantitative data collected during or following eruptions. The Baekdu volcano has experienced one massive eruption, also called the Millennium eruption, and several smaller eruptions have been recorded historically (Decker and Decker, 1991).

Previous research on the Baekdu volcano has included a study of the applicability of the geographic information system software LAHARZ (Jung *et al*., 2013), a simulation analysis of volcanic flow (Kim *et al*., 2014), and a simulation of ash eruption (Kim, 2011). However, in the previous study, there was no direct calculation of the hazard area caused by Lahar in the eruption of Baekdu volcano. Therefore further study is still required. We therefore aimed to estimate potential hazard zones due to lahar damage using the LAHARZ simulation and VEI. We performed two simulations: in the first, the lahar volume was predicted; and in the second, we measured the slope of each region and determined the weighted lahar ratio.

2. Study Area

The Baekdu volcano is located at 41°59′34″N, 128°04′39″E (Fig. 1) and its highest peak is 2,750 m a.s.l. The outer diameter of the outer ring surrounding the caldera (Cheon-Ji or Heaven Lake) is 4.4 km south–north by 3.7 km east–west; the lake has an area of 9.82 km2, an altitude of 2,189 m, a maximum depth of 374 m, and a volume of about 2 billion tons (Suh *et al*., 2013).

The Baekdu volcano was formed by a basaltic magma eruption about 150-100 million years ago,

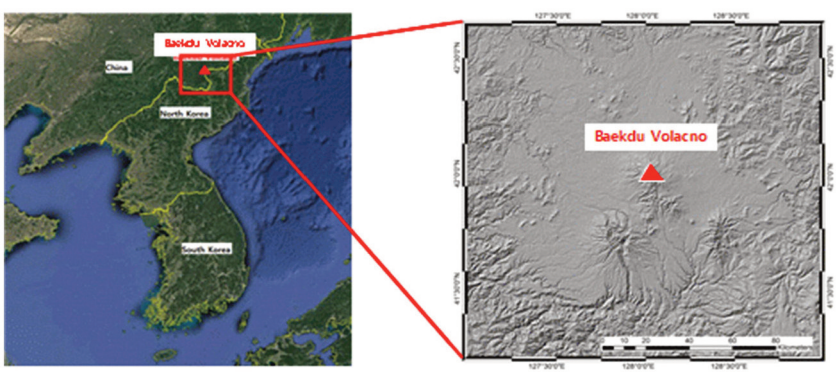

Fig. 1. Location of Baekdu Volcano, South Korea.

followed by subdivision of the volcanic body 600,000-10,000 years ago. The top of the mountain collapsed with a large eruption of pumice about 4,000-1,000 years ago, forming the caldera. The historical record of volcanic eruptions indicates large and small eruptions from the beginning of the 11th century to the beginning of the 20th century (Yun and Cui, 1996). Since the occurrence of a magnitude 7.3 earthquake in Wangcheng, China in June 2002, the frequency of earthquakes that signal imminent volcanic eruption has increased around the Baekdu volcano (Wu *et al*., 2005). On August 23, 2003, a magnitude 2.3 earthquake near Baekdu volcano caused a crack in the mountain slope, another precursor of volcanic eruption. A landslide occurred on September 8, 2004, due to a magnitude 3.7 earthquake near Baekdu volcano; in the same year, many trees were destroyed, apparently due to an eruption of toxic volcanic gas. Temperatures of Cheon-ji lake has increased, the contents of helium and hydrogen in volcanic gas have increased by more than 10 times, and the surrounding terrain has increased by more than 10 cm (Yun *et al*., 2012). In addition, the velocity difference between P and S waves around the Baekdu volcano indicates that there is an extensive magma chamber beneath the Baekdu volcano (Ri *et al*., 2016).

3. Method

In this study, we used the LAHARZ program to quantify the potential extent of lahar damage. The LAHARZ program was developed by analyzing the flow of 27 volcanoes in nine countries using digital elevation models (DEMs) and empirical Equations (1) and (2). The area of the volcanic advection was determined from the volume (V) of the volcano and the ratio of volcano height (H) to lahar horizontal distance (L), Cross section Area of lahar flow (A), area of lahar flows (B). Fig. 2 shows the areas calculated using Equations (1) and (2), varying the H/L ratio from 0.05

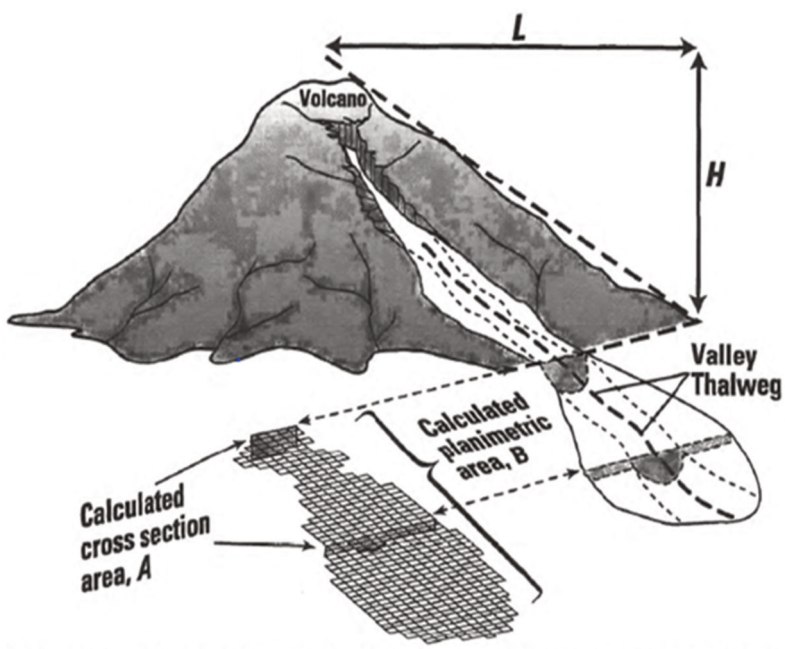

Fig. 2. Factors influencing volcanic flooding zones in the LAHARZ simulation program. (A) Cross section Area of lahar flow, given a volcano height (H) to lahar flow length (L) ratio of 0.05; (B) area of lahar flows, given an H/L ratio of 200 (Iverson *et al*., 1998).

to 200 (Iverson *et al*. 1998).

$$A = 0.05V^{\frac{2}{3}} \quad (1)$$

$$B = 200V^{\frac{2}{3}} \quad (2)$$

Because LAHARZ utilizes a relatively small number of input parameters, it is very effective for estimating approximate damage in cases where field survey data are insufficient or data acquisition is difficult. It is also useful for planning the evacuation of people near the volcanic area because it can quickly and easily estimate volcanic flood areas (Schilling, 1998). In this study, we simulated six water systems for two scenarios: constant volcanic flow rate and a flow rate that varies according to the slope. The LAHARZ algorithm consists of several steps Table 1), with the lahar flow determined by input variables at each step.

LAHARZ comprises a unidirectional algorithm that can calculate only one flow at a time. Therefore, we selected six flow directions for this study: two to the east, one to the north, two to the west, and one to the south. These flows were designated as East1, East2, North1, West1, West2, and South1, respectively (Fig. 3); their positions and coordinates are shown in Fig. 3. These points were selected from the outside of the PROXIMAL-HAZARD ZONE BOUNDARY, which showed irregular flow when the first volcanic eruption occurred. The lahar discharge volume was determined according to VEI; the volume corresponded to boundary values between VEI 3 and 7 (Table 2).

The first simulation assumed that the lahar flow was equal in all directions, and the volume of the specified lahar was therefore divided equally between the flows. In the second simulation, we assumed that the lahar volume would vary according to the slope of each water system. In order to calculate the slope at each point, the altitude of each point was measured and the slope was calculated using the altitude. Table 3 shows the altitude of each site and the ratio of lahar in the each simulation.

The following equation (3) was used to make the ratio of lahar parameter in 2nd simulation using altitude. Altitude (A), each point (n).

$$\frac{\frac{1}{An}}{\sum\frac{1}{An}} \quad (3)$$

Table 1. LAHARZ launch stage, input data, and parameters

Input data	Stage	Parameter
DEM	1. Create Surface Hydrology Grids	Fill Threshold, Stream Threshold
	2. Create a proximal hazard Zone Boundary	H/L Ratio Maximum Elevation
	3. Select Stream	Flow Direction
	4. Create lahar Inundation Zone	Lahar Volume

Table 2. Eruption volume and examples for varying volcanic explosivity index (VEI) values

VEI	Erupted Volume	Example
0	< 10,000 m^2	
1	> 10,000 m^2	Nyiragongo (2002)
2	> 1,000,000 m^2	Mt. Sinabung (2010)
3	> 0.01 km^2	Soufriere Hills (1995)
4	> 0.1 km^2	Eyjafyallajokull (2010)
5	> 1 km^2	Mt. St. Helens (1980)
6	> 10 km^2	Mt. Pinatubo, Philippines (1991)
7	> 100 km^2	Tambora (1815)
8	> 1000 km^2	Yellowstone (Pleistocene)

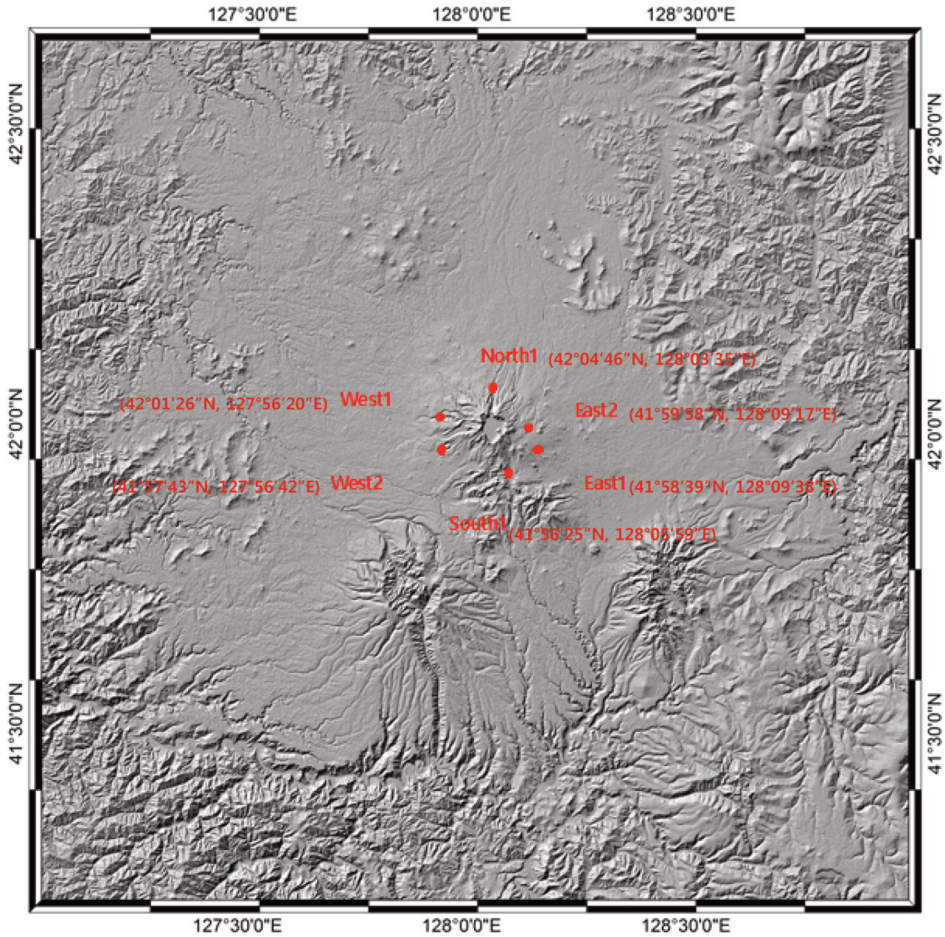

Fig. 3. Location of lahar starting point.

Table 3. Elevation of lahar starting point and its input lahar ratio

Point	Elevation (m)	Ratio of Lahar	
		1st Simulation	2nd Simulation
East1	2016	Each 16.67%	14.32%
East2	2048		14.23%
North1	1650		17.06%
West1	1504		19.19%
West2	1495		19.50%
South1	1792		15.71%

A total of 60 simulation results were obtained and plotted for the two simulations and six lahar volumes calculated from boundary values between VEI 3 and 7; the results were analyzed using Google Earth to determine the areas of simulated lahar damage.

4. Results

The number of pixels in the simulation results and the resolution of the DEM used in this study are summarized in Table 4. The first LAHARZ simulation assumed that lahar flow was uniform in all directions at the same rate. The north flow direction comprised a relatively large, flat area; and the south flow direction comprised a deep valley along the Yalu River. Thus, the northward-flowing lahar flowed through the water system and also escaped through a water system to the side. In comparison, the southward-flowing lahar was narrower and longer (Fig. 4). The results for the east and west lahar flows were similar to those for flows to

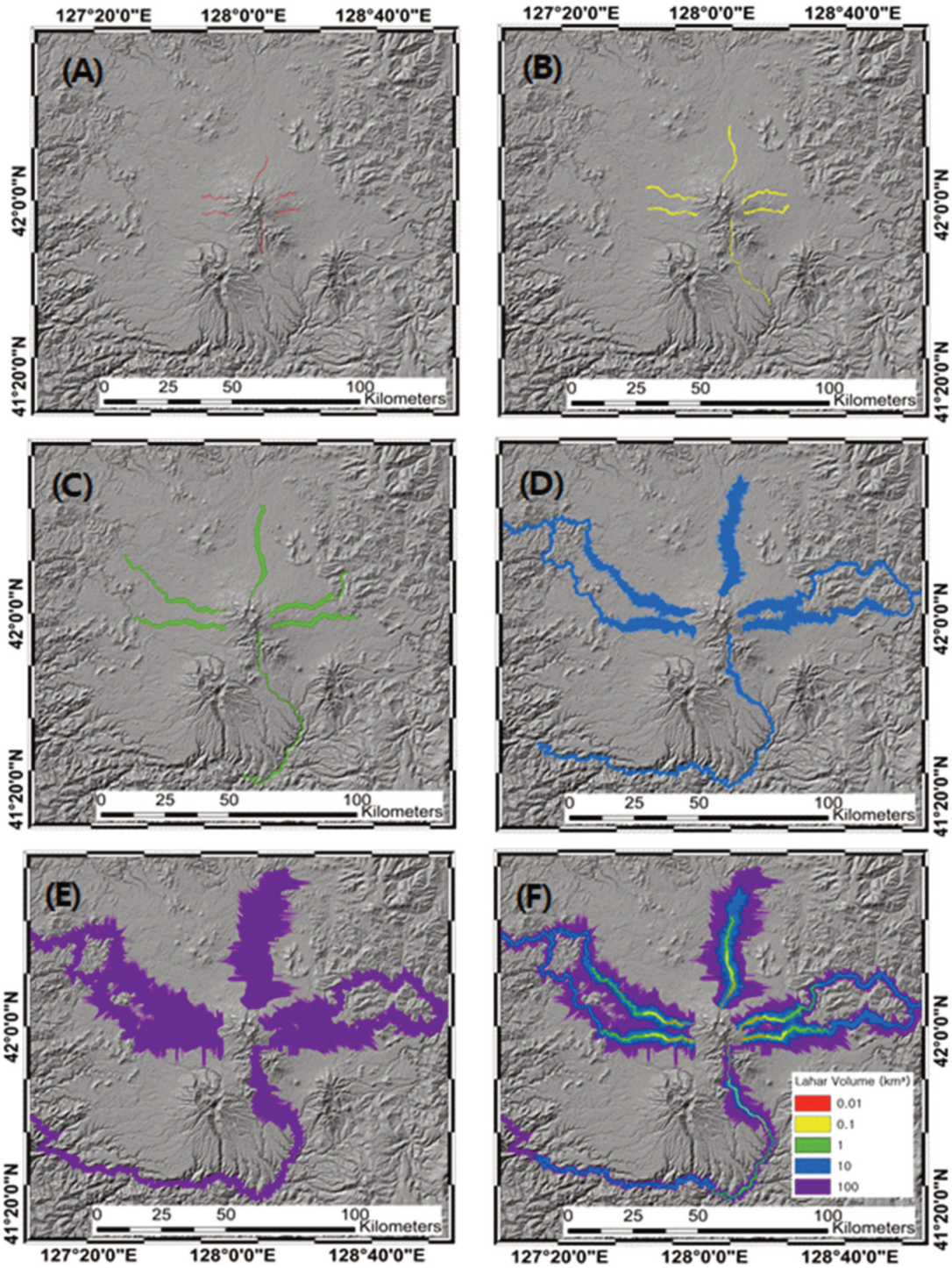

Fig. 4. Result of Simulation 1. (A) Volcanic explosivity index (VEI) = 3; (B) VEI = 4; (C) VEI = 5; (D) VEI = 6; (E) VEI = 7; (F) merged results from (A–E).

Table 4. Simulation result for Scenario 1 flooding area obtained using the LAHARZ software

VEI	Point	Pixel Count	Flooded Area (km²)	
3	East1	3130	2.817	16.898
	East2	3124	2.812	
	North1	3126	2.813	
	South1	3140	2.826	
	West1	3126	2.813	
	West2	3130	2.817	
4	East1	14520	13.068	78.339
	East2	14501	13.051	
	North1	14507	13.056	
	South1	14500	13.050	
	West1	14507	13.056	
	West2	14509	13.058	
5	East1	67304	60.574	363.548
	East2	67318	60.586	
	North1	67354	60.619	
	South1	67329	60.596	
	West1	67318	60.586	
	West2	67319	60.587	
6	East1	304618	274.156	1618.326
	East2	263665	237.299	
	North1	312408	281.167	
	South1	292584	263.326	
	West1	312451	281.206	
	West2	312414	281.173	
7	East1	769079	692.171	4650.777
	East2	616467	554.820	
	North1	1019410	917.469	
	South1	814871	733.384	
	West1	1014031	912.628	
	West2	933672	840.305	

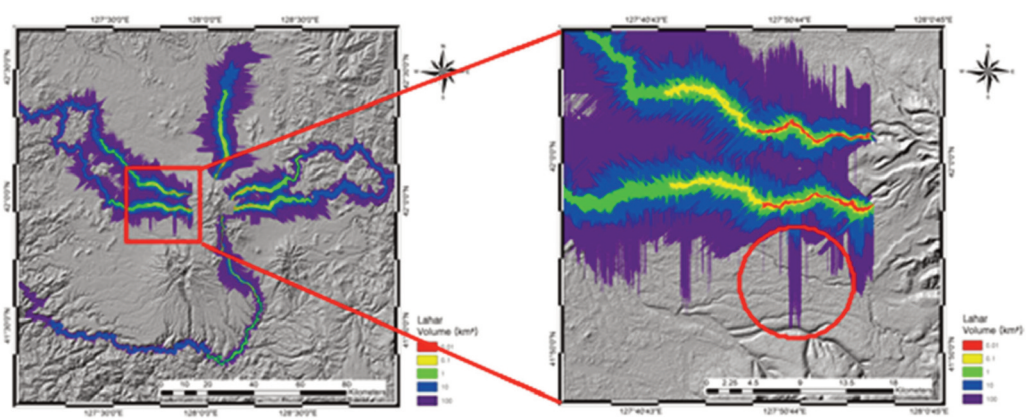

Fig. 5. Example of ragged edges in a LAHARZ simulation.

the north and south. The middle region of the study area is flat terrain; however, the simulated lahar flowed along the water system, which is surrounded by mountains. Therefore, the result was a narrow and long flow toward the end of the study area. In addition, an accurate flooding area was calculated using the number of pixels acquired through the results of the LAHARZ program (Table 4). Fig. 5 shows a region that protrudes abruptly from the lahar flow. This area corresponded to missing values in the DEM, due to an error in the LAHARZ program. These errors can be resolved using higher-resolution DEMs. In this study, we used 30 m SRTM DEMs; future studies should increase the DEM resolution (Munoz *et al*., 2009).

The assumption that the lahar flow was equal in all directions did not sufficiently represent natural phenomena. Therefore, in the second simulation, we obtained the slopes of each lahar starting point on the volcano, and distributed the lahar volume proportionally according to the slope. The results of this simulation are shown in Fig. 6 and the flooded area is described in Table 5.

Table 5. The result for Simulation 2 flooding area obtained using LAHARZ

VEI	Point	Pixel Count	Flooded Area (km2)	
3	East1	2818	2.536	16.871
	East2	2791	2.512	
	North1	3221	2.899	
	South1	3057	2.751	
	West1	3421	3.079	
	West2	3437	3.093	
4	East1	13088	11.779	78.224
	East2	12924	11.632	
	North1	14934	13.441	
	South1	14138	12.724	
	West1	15882	14.294	
	West2	15949	14.354	
5	East1	60642	54.578	362.871
	East2	60011	54.010	
	North1	69274	62.347	
	South1	65565	59.009	
	West1	73711	66.340	
	West2	73987	66.588	
6	East1	281400	253.260	1645.628
	East2	246205	221.585	
	North1	321572	289.415	
	South1	304321	273.889	
	West1	342109	307.898	
	West2	332868	299.581	
7	East1	727414	654.673	4704.440
	East2	580545	522.491	
	North1	1038461	934.615	
	South1	801307	721.176	
	West1	1079036	971.132	
	West2	1000393	900.354	

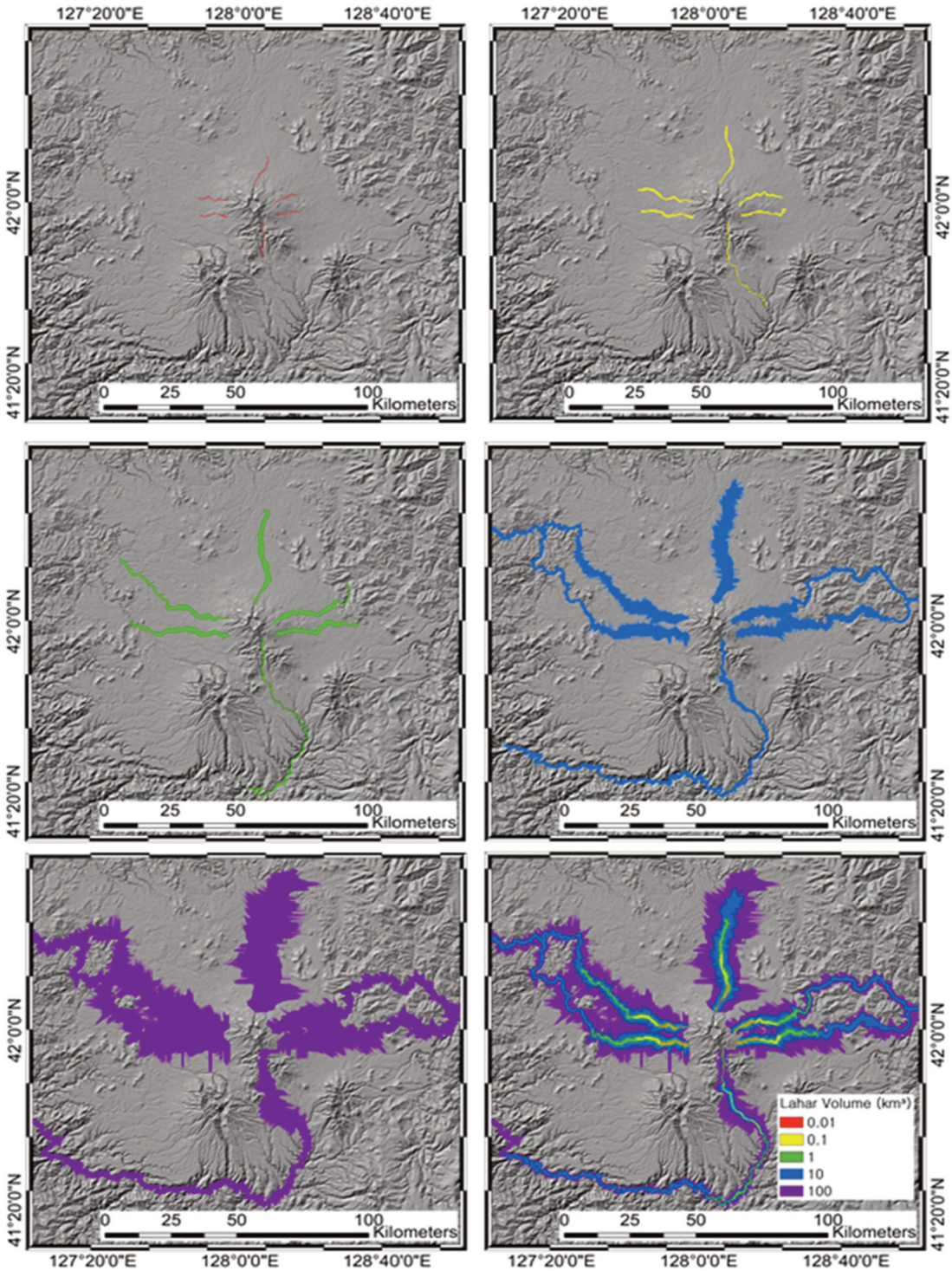

Fig. 6. Result of Simulation 2. (A) VEI = 3; (B) VEI = 4; (C) VEI = 5; (D) VEI = 6; (E) VEI = 7; (F) merged results from (A–E).

A comparison of the first simulation, using equal lahar flow in all directions; and the second simulation, in which lahar volume varies according to slope, showed that the lahar-flooded area varied due to terrain differences in the second simulation. In order to more easily compare the differences between the simulation 1 and simulation 2, we plotted graph (Fig. 7). The largest increase in affected area occurred in West2, where the flooded area was about 2.83% larger in the second simulation than in the first (Fig. 8). The greatest decrease occurred in East2, in which the flooded area was 2.44% smaller than in the first simulation (Fig. 9). Given the overall change in the total flooded area, these changes were relatively small. Changing the H/L ratio resulted in a travel distance increase or decrease of about 5%. To obtain further information about the influence of terrain on lahar flow, we extracted and analyzed these data using the Google Earth (Fig. 10).

At VEI values of 3 and 4, there was no direct lahar damage to residential areas. At VEI 5, however, the lahar began to flow into residential areas, affecting the Changbai Chinese autonomous Prefecture in China,

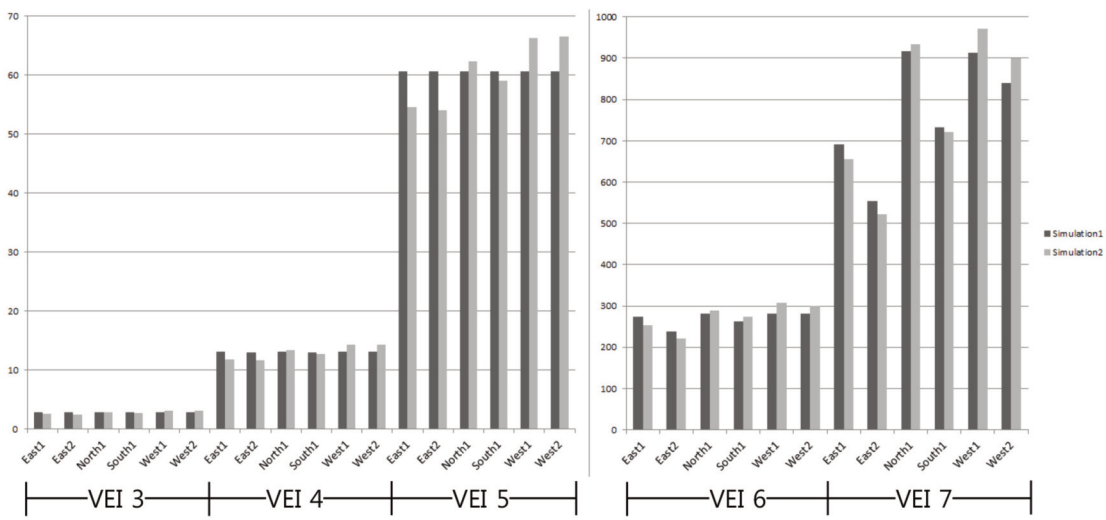

Fig. 7. Flooded area of lahar according to VEI at each point.

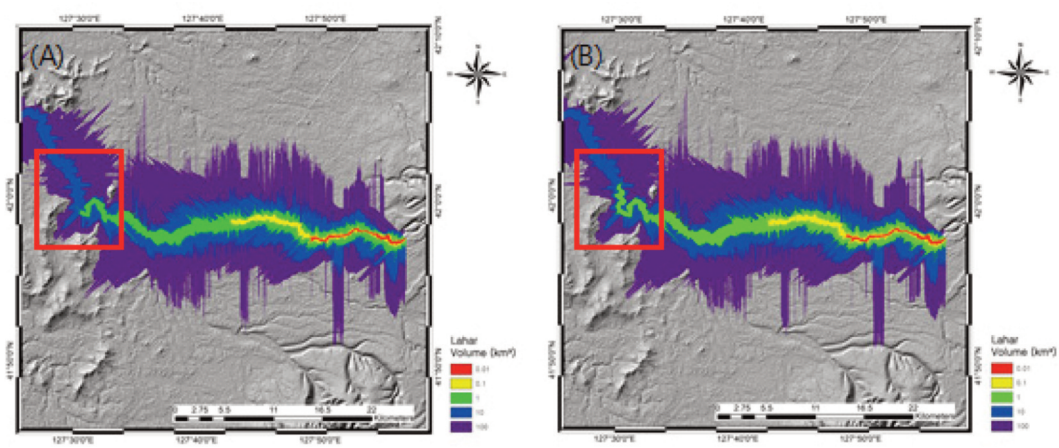

Fig. 8. Decreases in simulated lahar flow when lahar volume was (A) equal across all starting points and (B) varied according to slope.

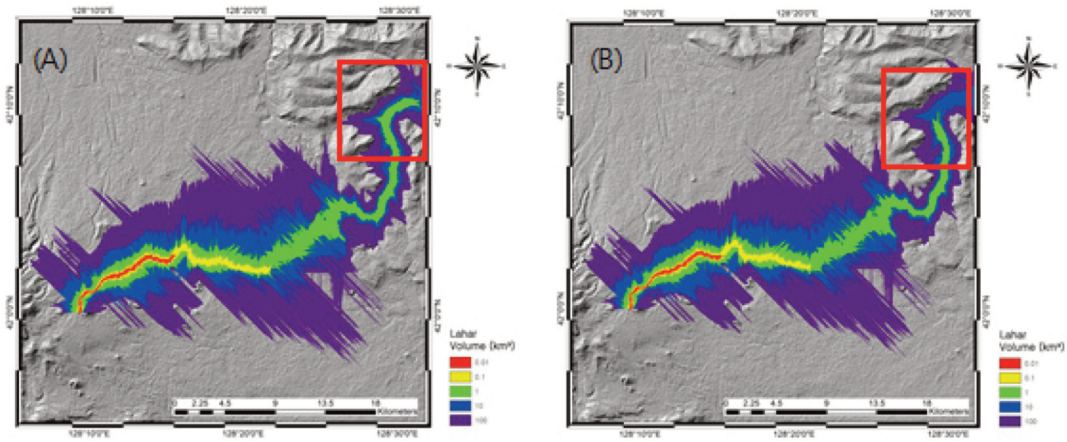

Fig. 9. Increases in simulated lahar flow when lahar volume was (A) equal across all starting points and (B) varied according to slope.

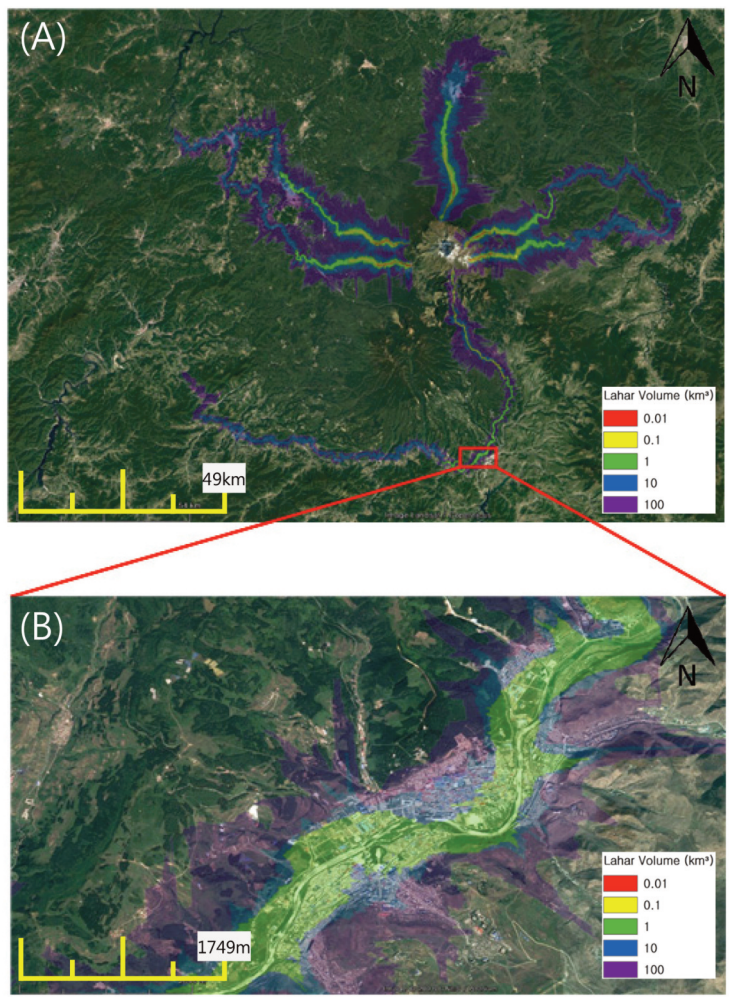

Fig. 10. Map of LAHARZ simulation2 result in this study analyzed using the Google Earth (A), At VEI 5, lahar flow affecting the Changbai Chinese autonomous Prefecture in China, Hyesan City in North Korea (B).

Hyesan City in North Korea, and Changxing County in Pudong County to the west. At VEI 6, the lahar was predicted to pass through numerous villages around the Yalu River to the south of the Baekdu volcano, including Kim Dae-dong and Kim Jeong-suk in North Korea. When VEI reached 7, all of the villages within a 100 km radius of the Baekdu volcano were included within the scope of the lahar.

5. Conclusion

In this study, we estimated the flooded area and estimated damage area due to lahar flow using six simulations of six water systems around the Baekdu volcano and 30 m SRTM DEM data. We applied the LAHARZ program, which has not been previously applied to calculate lahar damage zones around the Baekdu volcano. We further analyzed our simulation results using the commercial software Google Earth to quickly identify potential lahar damage areas. At each VEI increment, the total lahar volume increased by a factor of 10. However, the flooded area did not increase in proportional to the lahar volume. When VEI was increased from 3 to 4, the flooded area became about 4.64 times larger. However, when VEI was increased from 6 to 7, the flooded area became about 2.87 times larger. This result was due to differences in terrain, such that when lahar volume was large, flow extended over adjacent water systems as well as the water system designated as the primary flow direction in the simulation. Nevertheless, the topography in the East2 and North1 directions resulted in a 1.8-fold variation in flooding area, because the northward flow passes over flat terrain with no bends in the water system, leading to widespread lahar flow that affected a larger area.

Our results showed that the LAHARZ program contains errors that cannot be solved within the software. Irregularities in the simulation results may be addressed using high-resolution images; however, no study has been conducted on the effects of resolution on LAHARZ simulation errors. Because the unidirectional algorithm adopted by the LAHARZ program is designed to accommodate only one water system per simulation, it carries the disadvantage that flow extending to tributaries is not considered. To solve this problem, it is necessary to repeat the simulation for each tributary. In this study, we considered only one variable, the mountain slope; however, additional variables should be considered in future studies The results of the current study will be useful for effective preparation for imminent eruptions of the Baekdu volcano.

Acknowledgment

This research was supported by the National Research Foundation of Korea (NRF) grant funded by the Korea government (MSIP) (No. 2015M1A3A3A02 013416), The National Research Foundation of Korea (NRF) grant funded by the Korea government (MSIP) (No. 2017R1A2B4003258), Korea Meteorological Administration Research and Development Program under Grant KMIPA (2015-3071). And this study is supported by 2017 Research Grant from Kangwon National University.

References

Schilling, S.P., 1998. *LAHARZ: GIS programs for automated mapping of lahar-inundation hazard zones*, U.S. Geological Survey Open-File Report, no. 98-638.

Kim, N.S., 2011. An Analysis on Influence Area by the Simulation over Mt. Baekdu Eruption, *Journal of The Korean Association of Regional Geographers*, 17(3): 348-356 (in Korean with English abstract).

Decker, R.W. and B.B. Decker, 1991. *Mountains of fire : the nature of volcanoes*, Cambridge Cambridge University Press, USA.

Yun, S.H. and Z.X. Cui, 1996. Historical Eruption Records on the Cheonji Caldera Volcano in the Mt. Paektu, *Journal of the Korean Earth Science Society*, 17(5): 1-14 (in Korean with English abstract).

Yun, S.H. and J.H. Lee, 2012. Analysis of Unrest Signs of Activity at the Baegdusan Volcano, *The Journal of the Petrological Society of Korea*, 21(1): 1-12 (in Korean with English abstract).

Yun, S.H., C.K. Won, and M.W. Lee, 1993. Canozoic Volcanic Activity and Petrochemistry of Volcanic Rocks in the Mt. Peaktu Area, *Journal of the Geological Society of Korea*, 29(3): 274-279 (in Korean with English abstract).

Newhall, C., J.W. Hendley II, and P.H. Stauffer, 1997a. *The Cataclysmic 1991 Eruption of Mount Pinatubo, Philippines*, U.S. Geological Survey Fact Sheet 113-97, Vancouver, WA.

Newhall, C., P.H. Stauffer, and J.W. Hendley II, 1997b. *Lahars of Mount Pinatubo, Philippines*, U.S. Geological Survey Fact Sheet, 114-97, Vancouver, WA.

Wu, J., Y. Ming, and H. Zhang, 2005. Seismic activity at the Changbaishan Tianchi volcano in the summer of 2002, *Chinese Journal of Geophysics*, 48(3): 621-628 (in Chinese with English abstract).

Jung, K.J., H.J. Kim, S.H. Kim, and K.H. Lee, 2013. Application of LAHARZ for Lahar Modeling in Mt. Baekdusan, *Journal of the Korean Earth Science Society*, 34(6): 507-567 (in Korean with English abstract).

Suh, J.W., H.U. Yi, S.M. Kim, and H.D. Park, 2013. Prediction of the Area Inundated by Lake Effluent According to Hypothetical Collapse Scenaros of Cheonji Ground at Mt. Baekdu, *The Journal of Engineering Geology*, 23(4): 409-425 (in Korean with English abstract).

Munoz-Salinas, E., M. Castillo-Rodriguez, V. Manea, M. Manea, and D. Palacios, 2009. Lahar flow simulations using LAHARZ program: application for the Popocatépetl volcano, Mexico, *Journal of Volcanology and Geothernal Research*, 182(1-2): 13-22.

Kim, H.J., K.H. Lee, S.W. Kim, E.K. Choi, S.H. Yun, and S.H. Kim, 2014. Scenario Based Analysis of Lahar Simulation of Mt. Baekdu Using LAHARZ, *Journal of International Area Studies*, 18(3): 243-263 (in Korean with English abstract).

Ri, K.S., J.O.S. Hammond, C.N. Ko, H. Kim, Y.G. Yun, G.J. Pak, C.S. Ri, C. Oppenheimer, K.W. Liu, K. lacovino, and K.R. Ryu, 2016. Evidence for partial melt in the crust beneath Mt. Peaktu (Changbaishan), Democratic People's Republic of Korea and China, *ScienceAdvances*, 2(4): e1501513.